

Contact *amcilverny01@qub.ac.uk*

A. McIlvenny, D. Doria, H. Ahmed, P. Martin, S. Kar, M. Borghesi

Centre for Plasma Physics, School of Mathematics and Physics, Queen's University Belfast, Belfast BT7 1NN, United Kingdom

L. Romagnani

LULI, École Polytechnique, CNRS, Route de Saclay, 91128 Palaiseau Cedex, France

S. Williamson, P. McKenna

SUPA, Department of Physics, University of Strathclyde, Glasgow G4 0NG, United Kingdom

E.J. Ditter, O. Ettliger, G. Hicks, Z. Najmudin

The John Adam's Institute, Imperial College London South Kensington Campus, London, SW72AZ, United Kingdom

D. Neely, N. Booth

Central Laser Facility, Rutherford Appleton Laboratory, Oxfordshire OX11 0QX, United Kingdom

Introduction

Ion acceleration from high intensity ($>10^{18}\text{W}/\text{cm}^2$) lasers has been extensively explored using a variety of laser and target parameters as a means of generating high energy, short duration (ps) ion bursts. Most of the focus has been towards Target Normal Sheath Acceleration (TNSA) generating short pulses of 10s of MeV multi-species ions from the target bulk and rear contaminants¹. This is typically done using targets with thickness of a few microns, where ions are accelerated by the strong sheath field (order of TV/m) created by the hot electrons at the target surfaces.

Theoretical and numerical investigations suggest that for the next generation of lasers with higher intensities ($>10^{22}\text{W}/\text{cm}^2$) radiation pressure acceleration (RPA) will begin to dominate, potentially achieving ion energies in the 100's of MeV to GeV range². Recent studies have shown that RPA can become the dominant acceleration mechanism already at current intensities by careful control of the target thickness and polarization of the laser, as also observed on Gemini³.

The use of circularly polarized light can help reduce electron heating of the target maintaining target opacity for longer³. This allows more efficient coupling of the laser's radiation pressure to the irradiated target, and the subsequent acceleration of the target bulk.

Ion acceleration experiments routinely utilize absolutely calibrated detectors such as radiochromic film (RCF), CR-39 (Columbia Resin 39, a solid-state track detector) and TPS with Image plates (IP). Calibrations for these detectors exist up to 10s of MeV for protons and heavier ions^{5,6}. The main disadvantage of using image plates as the detector for a TPS are the long processing times required to obtain qualitative information as it is only after breaking vacuum and processing the IPs that you can obtain information on the energies achieved in a shot. These disadvantages can be overcome with the use of MicroChannel Plates (MCP), which provides a real-time response and can be operated without breaking the vacuum.

We report here on the calibration of a TPS – MCP assembly up to 21MeV/u (252MeV) for C^{6+} under conditions of relevance to ultrathin foils investigations similar to those reported in [3]. The calibration data was collected in a follow up experiment aiming to extend the previous dataset and to advance our understanding of radiation pressure acceleration, and its dependence on target thickness and laser polarization.

Experimental set-up

The north beam in TA3 was used, as seen in figure 1, in the double plasma mirror configuration to produce a contrast $>10^{12}$

in order to preserve the integrity of the foils; this reduces the amount of front surface expansion before the main pulse arrives providing a steep density gradient for the interaction. The beam passed through a quarter wave plate to alter the polarization between linear and circular. The beam was focused using the $f/2$ parabola and incident at 0° . This produced $\sim 6\text{J}$ on target and an intensity of $\sim 3.5 \times 10^{20}\text{W}/\text{cm}^2$. Amorphous carbon targets 2-100nm thick were shot and the polarization varied. The diagnostic set-up was optimized for the detection of high energy carbon ions and protons, as expected from bulk acceleration in the ultra-thin target regime. Thomson Parabola Spectrometers (TPS) were the main diagnostic and were placed at -9° , 0° and 4° degrees with respect to laser axis behind the target.

To make full use of the repetition rate of Gemini, Microchannel Plates (MCPs) were used within the TPS to record the particle spectra. A calibration for this detector was an objective for present and future use, as required in order to achieve quantitative information on the ion spectra.

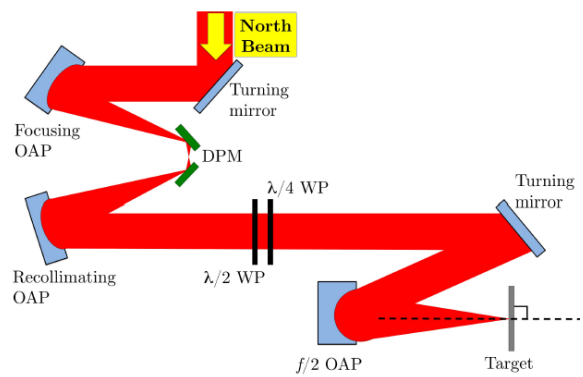


Figure 1: Double Plasma mirror and $f/2$ parabola set up⁴

Micro Channel Plate Detectors

A Microchannel plate acts as an electron multiplier to incident ionizing radiation and enhances the signal by a potential difference (PD) towards a phosphor screen. The fluorescence has a 10% decay time of less than 1ms and this is captured with a CCD with a longer exposure (typically 100ms) using the same trigger as the laser. The image can be obtained remotely and immediately after the shot and hence a measure of the maximum energy per species can be calculated almost instantly.

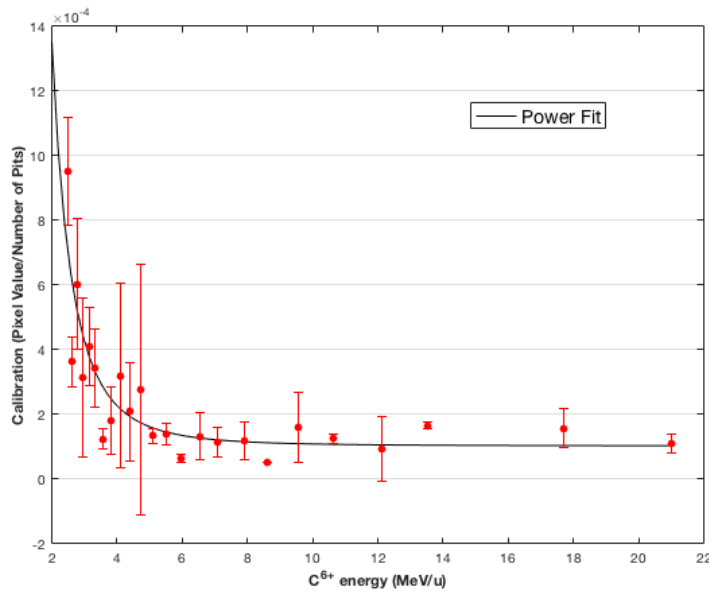


Figure 2: Calibration function for each energy bin for TPS 0° : A power function was fitted (see Table 1)

MCPs require a high vacuum ($>10^6$ mbar) to safely operate and a large PD (3-4kV), however this is typically smaller than the electric field for the TPS' electric field plates. The response of these detectors to this type of radiation has not been well characterized and a calibration is necessary for a quantitative characterization. The response is not necessarily expected to be linear against particle energy due to the large variance in the LET for the different energy ions produced in a single shot. In the context of our experimental program aimed at characterizing RPA, it is useful to extract an absolute energy spectrum in order to identify features associated with the acceleration mechanism, particularly in relation to the carbon ions from the target bulk. Typical TNSA spectra have an exponential decay spectrum following the Maxwellian electron temperature while spectral modulations may be indicative of RPA processes.

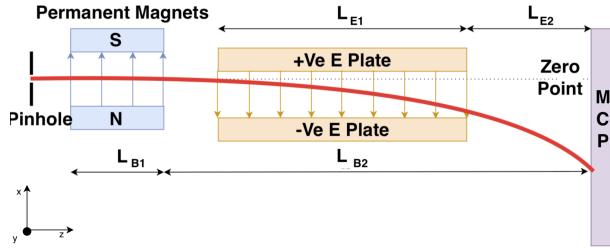


Figure 3: Top down view of Thomson Parabola Spectrometer Schematic and showing ion deflection – Labelled distances are displayed in Table 2

Three MCPs were used in this experiment, one for each of the TPSs. These were Hamamatsu MCPs of diameter 77mm (at -9° and 0°) and 33mm (at 4°) and the TPS schematic is seen in figure 3. Since the energy dispersion from the TPS magnet decreases as the energy increases, a larger diameter MCP allows for the use of a stronger magnet to increase the energy resolution for higher energy ions whilst also keeping more of the low energy ions on the screen. The off-axis TPS at larger angles can utilize weaker magnets to gain information for the lower energy ions as high energy ions are not typically seen off axis when shooting at normal incidence.

| Energy Range (MeV/u) | Fit |
|----------------------|---|
| 2-21 | $0.01257 \times \text{energy}^{-3.331} + 0.0001028$ |

Table 1: Calibration function fit

Using the information in table 1 along with the equations below, the vertical deflection (S_B) can be calculated (where r_L is the Larmor radius associated with the B field). This gives a measurement for the energy seen on the detector. The electric field separates the species and the deflection (S_E) is given by equation (2).

| Measurement | Value |
|--|---------|
| TCC \rightarrow Pinhole | 964.6mm |
| Pinhole size for calibration | 0.4mm |
| Pinhole \rightarrow Magnet | 67mm |
| Magnet \rightarrow Detector (L_{B2}) | 555mm |
| Magnet Width (L_{B1}) | 50mm |
| E Plate Width (L_{E1}) | 200mm |
| E Plate \rightarrow MCP (L_{E2}) | 335mm |
| B Field Strength (B) | 0.972T |
| E Field Strength (E) | 25kV/cm |

Table 2: Measurements used to calculate vertical and horizontal deflection for the 0° TPS

$$S_B = r_L - \sqrt{r_L^2 - L_{B1}^2} + \frac{L_{B1}L_{B2}}{\sqrt{r_L^2 - L_{B1}^2}} \quad (1)$$

$$S_E = \frac{qEL_{E1}}{mv_0^2} \left[\frac{L_{E1}}{2} + L_{E2} \right] \frac{r_L^2}{\sqrt{r_L^2 - L_{B1}^2}} \quad (2)$$

Together these produce a parabolic trace as seen in figure 5(a).

MCP Calibration

Slotted CR-39 (slot width of 1mm) was placed in front of the MCP on a shot (e.g. figure 4b). As the carbon ions stop in the 1mm thick CR-39, they could not reach the MCP through the CR-39. A segment of a parabolic trace will therefore be intercepted by the CR39, resulting in ‘‘shadows’’ on the MCP signal in correspondence of the CR-39 bars. A signal is produced on the MCP through the slotted gaps and at the edges of the gaps, the CCD pixel value and CR-39 carbon pit density can be directly compared. The parabolic trace of carbon ions is now composed of alternating MCP and CR-39 segments at different energies so that a calibration curve can be created using the data at each interface. The CR-39 was processed after the experiment by etching it in a 6M solution of NaOH at 85°C in short intervals

and an etched slot can be seen below in figure 4. Each slot was then imaged using a light microscope and the images stitched together. The pits could then be counted using ImageJ. The total pixel value for the width of the parabolic trace (using equations 1 and 2) is ‘binned’ using a Matlab code and this same resolution was applied to the CR-39. The number of pits within the same distance (equal to 1 pixel = 100 μ m) were then counted at each MCP – CR39 interface. This was then plotted against the energy at the interface and a function produced as seen in figure 2. For low energy/high LET carbon ions, their stopping distance (and Bragg peak) is situated within the detector. For higher energy particles, their Bragg peak would not be reached within the confines of the detector, and hence they deposit a smaller portion of their kinetic energy and subsequently produce a lower signal. In a typical ion spectrum, particle number also typically decreases with energy, e.g. according to a Maxwellian energy distribution.

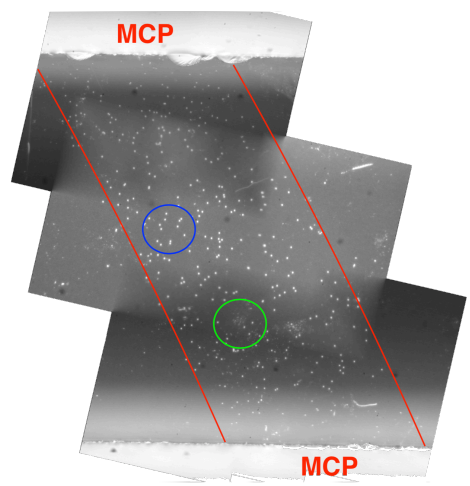


Figure 4: Mosaic image of CR-39 at x10 magnification showing the width of the parabolic ion trace (red lines) and the CR-39 – MCP interface at 4.1 MeV/u (top) and 4.4 MeV/u (bottom). The blue circle represents C^{6+} and green represents noise from damage particles

It is therefore expected that the response decreases for increasing energies as mentioned above which corresponds to the fitted power law⁷. At sufficiently high energies, the signal will become indistinguishable from the noise.

The uncertainties associated with each energy bin arise from the counting of the pits per energy bin and tend to arise due to small scale spectral modulations and detected only on the MCP or CR-39. At this point, the MCP image and CR-39 interface would not correspond to the same number of particles which can lead to an underestimate/overestimate of the number of particles in this energy region of the calibration.

A model is currently being prepared to describe the response of the detector to particles of varying LET radiation and to their penetration depth based on a similar set up⁸. This can be modelled with Monte Carlo simulations to see if the power law produces an accurate prediction for the detector response to higher energy particles.

Spectra

The calibration can then be applied to the CCD pixel value for each energy. Knowing the solid angle of the entrance pinhole of the TPS (in this case 118nSr) one can produce an absolutely calibrated spectrum in particle number per MeV per steradian. The noise of the detector is also shown in figure 6 alongside a C^{6+} spectrum. The maximum ion energy is then determined to be at the point when the ion signal trace can no longer be distinguished from the noise. The noise is measured as the signal of a parabolic trace on the detector alongside the carbon trace where there is no ion trace present (e.g. between protons and C^{6+} in figure 5a). The noise was then smoothed out and plotted as a

simple power law fit. As mentioned before, previous experiments (ref [3]) irradiated similar targets on Gemini but employed Image Plates in the TPS. Using MCPs and similar targets, we are able to reproduce quantitatively these spectra, which confirms the correctness of the calibration

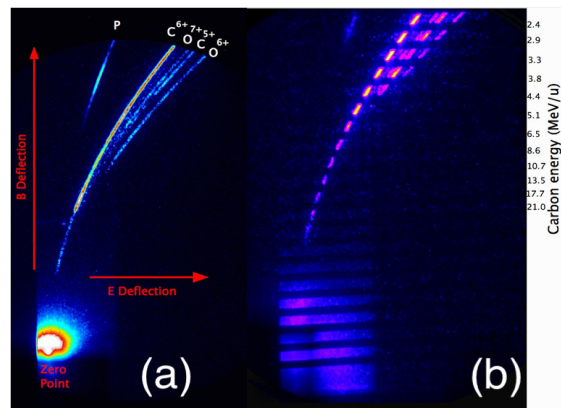


Figure 5 (a) MCP imaged on shot with Andor Neo CCD (false colour) (b) calibration shot using slotted CR-39 which the carbon passes through

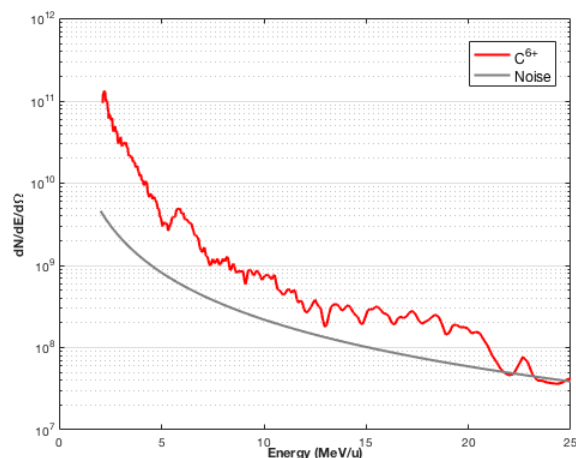


Figure 6: Spectra for a 15nm C foil with particle number/MeV/steradian plotted with the noise. Maximum energy is ~22MeV/u

Conclusions

The response of a Thomson Parabola Spectrometer – MCP assembly was calibrated for absolute particle number. It was calibrated up to 21 MeV/u, and, assuming the same power law fit, can be extended to higher energies. The response is best described using a power law. This has allowed for a calibrated spectrum to be produced for C^{6+} which is clearly a very important measurement for bulk ion acceleration from thin foils. Monte Carlo simulations will be performed to determine the scaling of the response to higher energy particles. The experiment shows that MCPs provide a promising method of detecting high energy carbon ions and producing spectra from high repetition rate, high power laser systems.

Acknowledgements

The authors acknowledge facility access provided by the Science and Technology Facility Council and grant support from the Engineering and Physical Sciences Research Council. The authors also acknowledge support from the laser and technical staff and target fabrication group at the Rutherford Appleton Laboratory.

References

1. Andrea Macchi, Marco Borghesi, and Matteo Passoni. Rev. Mod. Phys. **85**, 751 2013
2. Esirkepov *et al* Phys. Rev. Lett. **92**, 175003
3. C. Scullion *et al* Phys. Rev. Lett. **119**, 054801 2017
4. C. Scullion, *Investigations of ion acceleration from solid targets driven by ultrashort laser pulses*, PhD Thesis, QUB 2016
5. A. Mančić *et al* Review of Scientific Instruments **79**, 073301 (2008)
6. D. Doria *et al* Review of Scientific Instruments **86**, 123302 (2015)
7. T.W. Jeong *et al*, Review of Scientific Instruments **87**, 083301 (2016)
8. R. Prasad *et al* Nuclear Instruments and Methods in Physics Research A **623** 712–715. (2010)